PLOS COMPUTATIONAL BIOLOGY

RESEARCH ARTICLE

A mechanistic modeling framework reveals the key principles underlying tumor metabolism

Shubham Tripathi[1,2], Jun Hyoung Park[3], Shivanand Pudakalakatti[4], Pratip K. Bhattacharya[4], Benny Abraham Kaipparettu[3,5], Herbert Levine[2]*

1 PhD Program in Systems, Synthetic, and Physical Biology, Rice University, Houston, Texas, United States of America, **2** Center for Theoretical Biological Physics and Department of Physics, Northeastern University, Boston, Massachusetts, United States of America, **3** Department of Molecular and Human Genetics, Baylor College of Medicine, Houston, Texas, United States of America, **4** Department of Cancer Systems Imaging, The University of Texas MD Anderson Cancer Center, Houston, Texas, United States of America, **5** Dan L. Duncan Cancer Center, Baylor College of Medicine, Houston, Texas, United States of America

* h.levine@northeastern.edu

Citation: Tripathi S, Park JH, Pudakalakatti S, Bhattacharya PK, Kaipparettu BA, Levine H (2022) A mechanistic modeling framework reveals the key principles underlying tumor metabolism. PLoS Comput Biol 18(2): e1009841. https://doi.org/10.1371/journal.pcbi.1009841

Editor: Melissa L. Kemp, Georgia Institute of Technology and Emory University, UNITED STATES

Received: April 8, 2021

Accepted: January 15, 2022

Published: February 11, 2022

Data Availability Statement: All relevant data are within the manuscript and its Supporting Information files.

Funding: This work was supported by the National Science Foundation (https://www.nsf.gov/) grant no. PHY-2019745 (H. L.), National Institutes of Health (https://www.nih.gov/) grants nos. CA253445 and CA234479 (B. A. K.), Department of Defense grant no. W81XWH-18-1-0714 (B. A. K.), National Institute of Biomedical Imaging and

Abstract

While aerobic glycolysis, or the Warburg effect, has for a long time been considered a hallmark of tumor metabolism, recent studies have revealed a far more complex picture. Tumor cells exhibit widespread metabolic heterogeneity, not only in their presentation of the Warburg effect but also in the nutrients and the metabolic pathways they are dependent on. Moreover, tumor cells can switch between different metabolic phenotypes in response to environmental cues and therapeutic interventions. A framework to analyze the observed metabolic heterogeneity and plasticity is, however, lacking. Using a mechanistic model that includes the key metabolic pathways active in tumor cells, we show that the inhibition of phosphofructokinase by excess ATP in the cytoplasm can drive a preference for aerobic glycolysis in fast-proliferating tumor cells. The differing rates of ATP utilization by tumor cells can therefore drive heterogeneity with respect to the presentation of the Warburg effect. Building upon this idea, we couple the metabolic phenotype of tumor cells to their migratory phenotype, and show that our model predictions are in agreement with previous experiments. Next, we report that the reliance of proliferating cells on different anaplerotic pathways depends on the relative availability of glucose and glutamine, and can further drive metabolic heterogeneity. Finally, using treatment of melanoma cells with a BRAF inhibitor as an example, we show that our model can be used to predict the metabolic and gene expression changes in cancer cells in response to drug treatment. By making predictions that are far more generalizable and interpretable as compared to previous tumor metabolism modeling approaches, our framework identifies key principles that govern tumor cell metabolism, and the reported heterogeneity and plasticity. These principles could be key to targeting the metabolic vulnerabilities of cancer.

Engineering grant no. EB031217 (P. K. B.), Department of Defense – Prostate Cancer Research Program – Idea Development Award (PC200641 to P. K. B.), Melanoma Research Alliance-Pilot grant (P. K. B.), and the CPRIT Computational Cancer Biology Training Program Postdoctoral Fellowship (RP170593 to S. P.). The funders had no role in study design, data collection and analysis, decision to publish, or preparation of the manuscript.

Competing interests: The authors have declared that no competing interests exist.

Author summary

Tumor cells exhibit heterogeneity and plasticity in their metabolic behavior, relying on distinct nutrients and metabolic pathways, and switching to reliance on different pathways when challenged by an environmental change or a drug. While multiple previous studies have focused on identifying metabolic signatures that can distinguish tumor cells from non-tumorigenic ones, frameworks to analyze the metabolic heterogeneity in tumors have been lacking. Here, we present a mechanistic mathematical model of some of the key metabolic pathways active in tumor cells and analyze the steady state behaviors the model can exhibit. We find that the rate of ATP use by tumor cells can be a key determinant of the metabolic pathway via which tumor cells utilize glucose. We further show that tumor cells can utilize different pathways for satisfying the same metabolic requirements, and explore the implications of such behavior for the response of tumor cells to drugs targeting tumor metabolism. At each step, we discuss how our model predictions fit within the context of experimental observations made across tumor types. The present modeling framework represents an important step towards reconciling the wide array of experimental observations concerning tumor metabolism, and towards a more methodical approach to targeting tumors' metabolic vulnerabilities.

Introduction

Proposed as an emerging hallmark of cancer nearly a decade ago [1], metabolic reprogramming has now entered into the limelight of cancer biology as a key feature of tumor cells across cancer subtypes, with multiple therapeutic implications [2]. Aerobic glycolysis, commonly known as the Warburg effect [3], characterized by increased glucose uptake most of which is excreted out as lactate even under normoxic conditions, has been synonymous with cancer cell metabolism for nearly a century. Studies carried out over the past decade have however revealed a more complex picture—there exists widespread intra-tumoral heterogeneity not only in the way tumor cells utilize glucose but also in the activities of the various other metabolic pathways in tumor cells. Further, tumor cells at different stages of metastatic progression exhibit different metabolic phenotypes and metastases growing in distinct organs can also exhibit differences in their metabolic activity [4,5]. Understanding the mechanistic basis of metabolic heterogeneity in different contexts will be key to the design of anti-cancer metabolic therapies.

A mechanistic modeling framework to understand the mechanistic underpinnings of tumor metabolic heterogeneity has been lacking. Multiple previous studies have relied upon constraint-based models such as flux balance analyses, often involving genome-scale metabolic models, to simulate the metabolic response of tumor cells and to identify the metabolic vulnerabilities (reviewed in [6]). Among the studies focused on explaining the Warburg effect, Vazquez *et al.* [7] showed that a switch to aerobic glycolysis can maximize the rate of ATP production by cancer cells under high glucose uptake while Shlomi *et al.* [8] have shown that under a solvent capacity constraint, the Warburg effect maximizes the rate of biomass production in cancer cells. Constraint-based modeling has been a popular approach for identifying anti-cancer targets [9–11] and for proposing cancer-specific metabolic signatures [12–15]. The analyses in these studies do not predict the widespread heterogeneity in the metabolic profiles of cancer cells in the primary tumor and of tumor cells at different stages of metastatic disease progression, mainly due to the involvement of a global objective function that all tumor cells must optimize. Further, the frameworks in these studies do not connect the metabolic

heterogeneity in tumor cells to the heterogeneity in other phenotypic states such as cell migration. While mechanistic models of tumor metabolism are more suited to addressing the questions concerning metabolic heterogeneity, past analysis has instead focused on fitting detailed models to a specific experimental setup [16] instead of identifying the general principles underlying tumor metabolism.

Recently, Jia *et al*. have put forth a systems-level analysis of coupled gene regulatory networks and metabolic pathways to describe metabolic heterogeneity and plasticity in tumor cells [17]. The study shows that cancer cells can switch between different metabolic states in response to changes in the activities of master regulators such as AMPK and HIF-1. However, the modeling approach therein is too coarse-grained to answer some interesting questions relating to the flux through different reactions in the metabolic pathways and to predict the detailed cellular response to perturbations in the activities of specific enzymes.

Here, we construct a mechanistic model which incorporates the key metabolic reactions that have been shown to be active in cancer cells. Instead of relying on a stoichiometric modeling framework such as flux balance analysis [18], we write down detailed mathematical equations describing the kinetics of different enzymatic reactions. The resultant system of ordinary differential equations can be numerically integrated to determine the steady state of the metabolic system. We show that the preference for aerobic glycolysis increases the flux through the anabolic pathways that use glycolytic intermediates as substrates, thereby facilitating fast proliferation. This results from the low ATP production when glucose is excreted out as lactate as compared to when glucose enters the TCA cycle as pyruvate. The rate of ATP consumption in cancer cells, which can vary with other cellular phenotypic properties, can thus modulate the preference of cancer cells for aerobic glycolysis versus oxidative phosphorylation. Next, we explore how the relative dependence of cancer cells on glucose and glutamine and the relative availability of these nutrients in the microenvironment can affect the metabolic profiles of tumor cells. We further use the model to predict the changes in the metabolic and gene expression profiles of melanoma cells under treatment with a BRAF inhibitor that can suppress glutamine uptake. Finally, we discuss how different experimental observations relating to cancer cell metabolism fit within the context of our modeling framework.

Results

Developing a mechanistic framework to model tumor metabolism

Our goal, in this study, is to explore the range of dynamical behaviors that can be exhibited by a new mathematical model which incorporates the critical aspects of tumor metabolism. We then analyze if the observed model behaviors can qualitatively explain any of the reported metabolic behaviors of tumor cells. This approach is in contrast to previous mechanistic modeling approaches that focus on fine tuning model parameters so that the model behavior is in agreement with the observations from a specific experimental setup (see, for example, Roy and Finley [16]), and allows us to develop a framework that can be utilized to analyze the metabolic behavior of tumor cells across cancer types and in different environments. The present framework is motivated by the success of a similar strategy in modeling the phenotypic heterogeneity and plasticity arising from gene regulatory networks [19,20].

Our model of tumor metabolism was constructed using the information available from the literature regarding the enzymatic reactions involved in key metabolic pathways active in tumor cells. These include glycolysis, the TCA cycle, oxidative phosphorylation, and glutaminolysis. A similar approach—obtaining the subset of cancer-specific metabolic reactions from the generic set of human metabolic reactions—has been popular for the construction of genome-scale models of tumor metabolism [9,12,13]. Here, instead of choosing the cancer-

specific metabolic reactions on the basis of cancer cell proteomics [9,12] or gene expression data [13], we chose the metabolic pathways for analysis on the basis of the available literature on tumor metabolism (reviewed in [21]). The dynamics of the concentrations of different metabolites in our setup were modeled using ordinary differential equations. The mathematical expressions describing the activities of the different enzymes and the relevant kinetic parameters were taken from the literature [22–26]. Oxidative phosphorylation and the electron transport chain reactions were treated using a simplified model proposed previously by Nazaret *et al.* [27]. Upregulation and downregulation of levels of different enzymes were modeled by changing the reaction velocity (V_{max}) for the enzyme by a multiplicative factor. The differential equations in the modeling setup (included in the S1 Text) were integrated numerically to determine the steady state model behavior. In the present study, our overall focus was on the maintenance of large anabolic fluxes to drive fast cell proliferation in different contexts. The baseline model description does not concern itself with the maintenance of redox homeostasis in tumor cells under varying conditions, which could be a key contributor to tumor cell survival. Therefore, we did not include two key pathways involved in redox homeostasis: the glycerol-3-phosphate shuttle [28] and the malate-aspartate shuttle [29]. Both these pathways help maintain a high NAD^+: NADH ratio in the cytoplasm for continued operation of the glycolytic chain of reactions. Here, we mimicked the overall functional effect of the two redox shuttles by fixing the cytoplasmic NAD^+: NADH ratio to a constant value. Moreover, the present model is applicable to scenarios wherein the carbon substrate availability for anabolic reactions is the limiting factor, not the redox capability of tumor cells (as is the case in Luengo *et al.* [30], for example) In a later section, we show how the baseline model may be extended to describe the case wherein cellular redox capability limits rapid cell proliferation.

A key challenge in the mechanistic modeling of cell metabolism is the unavailability of many of the mathematical expressions describing the kinetic behavior of different enzymes and the relevant kinetic parameters. In such cases, we made reasonable assumptions based on Michaelis-Menten kinetics [31]. Even in cases where the relevant kinetic information is available, the data obtained from different sources are often not compatible [23]—the expressions describing enzyme kinetics as well as the relevant kinetic parameters used in the present study were obtained from multiple previous studies [22–26] which themselves relied on results from experiments conducted in different tissue types, in cells from different species, and under a varied set of conditions. The incompatibility of the kinetic parameters can lead to scenarios wherein the different metabolic fluxes do not balance, and the system does not exhibit a non-trivial bounded steady state. To address this issue, some of the kinetic parameters obtained from previous studies were manually adjusted until the model exhibited a bounded steady state. This constraint on the model kinetic parameters is similar to the constraint on the steady state metabolic fluxes commonly imposed during flux balance analyses [18]. A more detailed discussion of the assumptions underlying model construction is included in the S1 Text. MATLAB code used to simulate the model behavior is available online (https://github.com/st35/cancer-metabolism). The MATLAB code files include the values of the different kinetic parameters in the model and the mathematical expressions used to describe the kinetics of the various enzymes. Note that the present modeling framework is not being put forth as an alternative to genome-scale metabolic models which allow for a global analysis of the role of different enzymes and metabolic pathways in tumor metabolism. Instead, the focus of the present model is on understanding the more microscopic picture—the role of metabolic feedback loops and of different enzymes in specific contexts. The model sacrifices completeness for interpretability and mechanistic insight.

In the following subsections, we discuss the behaviors exhibited by our metabolic model and their relevance to cancer biology.

Inhibition of phosphofructokinase by ATP can drive the preference for aerobic glycolysis in fast proliferating cells

As shown in Fig 1A, intermediate metabolites generated during the multi-step process that converts glucose to pyruvate are used in key anabolic processes required for cell division [21]. These include the ribose synthesis pathway, crucial for nucleotide synthesis, and the phospholipids synthesis pathway. A large flux through both these pathways is likely to facilitate fast proliferation. To determine how this may be achieved, we simulated the dynamics of the glycolysis pathway along with the first reactions in the ribose synthesis and the phospholipids synthesis pathways. Fig 1B shows that the steady state flux through both ribose synthesis and phospholipids synthesis pathways can be increased by increasing the rate of glucose uptake. To obtain this result, we have assumed that all the pyruvate that is generated from the glucose taken up by a cell is utilized via some metabolic process inside the cell and that any ATP produced during such a process is also used up, thereby keeping constant the concentration of ATP inside the cell. The pyruvate generated from glucose can have two primary fates (Fig 1A). On the one hand, lactate dehydrogenase (LDH) can convert pyruvate into lactate which is then excreted out of the cell. On the other hand, the pyruvate can enter the mitochondria where it is converted to acetyl coenzyme A (acetyl-CoA) by the enzyme pyruvate dehydrogenase (PDH) and further oxidized via the TCA cycle. The rate of glucose uptake in tumor cells can be increased by increasing the activity of either of the two enzymes (Fig 1C). The increased

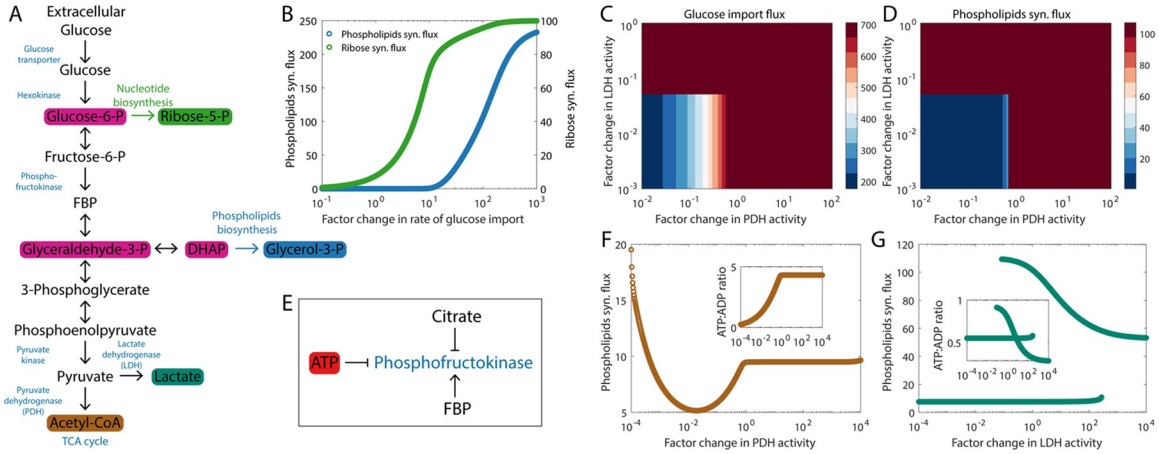

Fig 1. High ATP production during oxidative phosphorylation can drive a preference for aerobic glycolysis in fast proliferating cells. (A) Reactions in the glycolytic pathway and key anabolic processes that use glycolytic intermediates as substrates. The pyruvate generated at the end of glycolysis can either be excreted out as lactate or enter the TCA cycle as acetyl-CoA. (B) Increased glucose uptake can drive large fluxes through the ribose synthesis pathway and through the phospholipids synthesis pathway. (C) Increasing the activity of pyruvate dehydrogenase (PDH), lactate dehydrogenase (LDH), or both can increase the glucose uptake. (D) The phospholipids synthesis flux increases upon the upregulation of PDH, LDH, or both. In (C) and (D), we have assumed that the ATP concentration in the cytoplasm remains constant despite the higher ATP production per glucose molecule when glucose is allowed to enter the TCA cycle by upregulating PDH activity. (E) Different metabolites that can modulate the enzymatic activity of phosphofructokinase (PFK). FBP: fructose-*1, 6*-biphosphate. (F) Variation of the phospholipids synthesis flux with an increase in PDH activity (while keeping LDH activity fixed). (G) Variation of the phospholipids synthesis flux with an increase in LDH activity (while keeping PDH activity fixed). The insets in (F) and (G) show how the ATP:ADP ratio varies in each case. The bistability in the phospholipids synthesis flux as the LDH activity is varied arises from a positive feedback loop—fructose-1, 6-biphosphate, the product of PFK's enzymatic activity, can allosterically activate the enzyme (see panel E). In panels C and D, the bistability shows up as a very sharp change in the fluxes with increasing LDH activity. Fluxes are in units of mM h^{-1} (millimolar per hour) and are shown at steady state.

https://doi.org/10.1371/journal.pcbi.1009841.g001

glucose uptake in turn increases the flux through the phospholipids synthesis pathway (Fig 1D). The symmetry between increasing glucose uptake and the phospholipids synthesis flux via increased lactate excretion and via increased flux through the TCA cycle, apparent in Fig 1C and 1D, is broken when the rates of ATP production in the two processes are taken into consideration (Fig 1E–1G). If the carbon taken in as glucose is excreted out as lactate, *2* ATP molecules per molecule of glucose are produced. Using the glucose carbon to drive the TCA cycle followed by oxidative phosphorylation can generate *30–32* molecules of ATP per glucose molecule [32]. At a fixed rate of ATP consumption by the cell, using a large fraction of the glucose taken up by the cell to drive the TCA cycle can lead to increased ATP accumulation in the cytoplasm (see inset in Fig 1F) which will inhibit the glycolytic enzyme phosphofructokinase (PFK) (Fig 1E), shutting down glucose uptake [33] and driving down the phospholipids synthesis flux (Fig 1F). Excreting out the glucose carbon as lactate, on the other hand, can limit the ATP-mediated downregulation of PFK activity (see inset in Fig 1G), thereby maintaining a high phospholipids synthesis flux (Fig 1G) which would help maintain fast proliferation rates. The high lactate production and low TCA cycle flux even under normoxic conditions characterizes the well-known Warburg effect. The high phospholipids synthesis flux with the Warburg effect (shown in Fig 1E) offers a possible explanation for the preference for the Warburg effect seen in rapidly proliferating tumor cells across cancer types.

Varying ATP requirements can drive heterogeneity in the metabolic phenotype exhibited by tumor cells

In the previous section, we have shown that the inhibition of PFK due to the accumulation of excess ATP (generated by allowing glucose-derived pyruvate to enter the TCA cycle) can downregulate anabolic processes including phospholipids synthesis. We propose that this could be the reason many fast proliferating cells exhibit the Warburg effect. The hypothesis implies that modulation of the rate of ATP consumption in cells can change which metabolic phenotype will lead to a large flux through anabolic processes and thus facilitate fast proliferation. Fig 2A shows that the metabolic phenotype that maximizes the flux through the phospholipids synthesis pathway can change as the rate of ATP consumption by tumor cells changes. At low, basal rates of ATP consumption, the high lactate secretion, low TCA cycle flux (high LDH, low PDH) metabolic phenotype is needed for driving a large flux through the phospholipids synthesis pathway. A switch to a phenotype with high TCA cycle flux (high PDH) will shut down this key anabolic process. However, in cells that consume ATP at very high rates, for example, in metastasizing cancer cells that are actively migrating through the extracellular matrix [34], ATP will not accumulate to concentrations high enough to inhibit PFK activity even when large amounts of ATP are produced per glucose molecule via the TCA cycle. These cells can thus sustain fast proliferation rates while not exhibiting the Warburg effect. Difference in ATP consumption by cells at different stages of metastasis can thus contribute towards the differences in the metabolic profiles of tumor cells at distinct stages of metastasis. Note that in Fig 2A, we have assumed that there is sufficient oxygen available for ATP generation via the TCA cycle followed by oxidative phosphorylation. When the oxygen supply is limited (as is often the case in the interior of solid tumors), cells have to rely solely on converting glucose to lactate for ATP production (anaerobic glycolysis). In such a scenario, the rate of lactate production will be higher in cells with higher rates of ATP consumption (Fig 2B).

A connection between ATP consumption by tumor cells and their metabolic phenotype was recently demonstrated by te Boekhorst *et al.* [35]. They observed that the stabilization of HIF1 (which downregulates PDH activity) in 4T1 mouse breast cancer cells decreased the oxygen consumption rate (OCR), as expected, but surprisingly did not significantly increase the

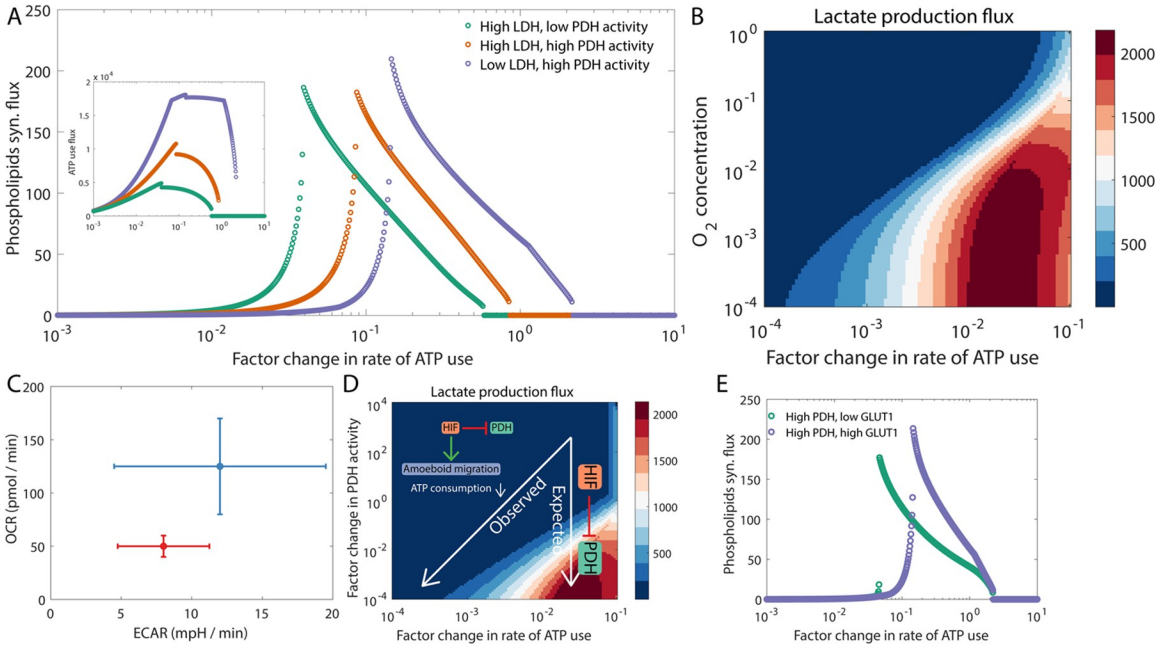

Fig 2. Rate of ATP consumption by tumor cells can modulate the preference for aerobic glycolysis versus oxidative phosphorylation. (A) The regime that maximizes the phospholipids synthesis flux depends on the rate of ATP consumption. The inset shows that the flux through pathways that consume ATP is maximized when the activity of PDH is high, i.e., when most of the glucose carbon enters the TCA cycle. (B) The rate of lactate production by tumor cells can depend not only on the availability of oxygen in the microenvironment but also on the rate of ATP consumption. (C) Change in the metabolic profile of 4T1 cells upon HIF1 stabilization (red) as compared to the control (blue). The behavior shown is representative of that reported by te Boekhorst *et al.* [35] (see *Fig 5E* therein). ECAR: extracellular acidification rate, which correlates positively with the rate of lactate excretion by cells. OCR: oxygen consumption rate, which correlates positively with the flux through the TCA cycle / oxidative phosphorylation pathway. (D) Change in the metabolic profile of cells upon HIF1 stabilization (which inhibits PDH activity) as predicted by our model. The change labeled as expected is when the migratory phenotype (and the rate of ATP consumption) remains unchanged upon HIF1 stabilization. The change labeled as observed is when HIF1 stabilization is accompanied by a switch from actin-driven migration to amoeboid migration [35] which decreases the rate of ATP consumption during cell migration. (E) Under high PDH activity and very high ATP consumption rate, GLUT1 up-regulation can increase the phospholipids synthesis flux. Fluxes are in units of mM h^{-1} (millimolar per hour) and are shown at steady state. The discontinuities in panels A and E arise from the bistability caused by the positive feedback from the allosteric activation of PFK by fructrose-1, 6-biphosphate (see Fig 1E).

https://doi.org/10.1371/journal.pcbi.1009841.g002

rate of lactate production (Fig 2C). The decrease in OCR is indicative of a decrease in the flux through the TCA cycle. Our model predicts that this can happen if ATP consumption by tumor cells also decreases along with the downregulation of PDH activity upon HIF1 stabilization (Fig 2D). This is indeed true in the case of 4T1 cells—upon DMOG treatment (which stabilizes HIF1), 4T1 cells underwent a change in their mode of migration from an actin-driven mode to an amoeboid mode involving fluid-filled, blebbing protrusions with no actin involvement [35]. ATP consumption in the actin-driven mode of cell migration is much higher as compared to that in the cell migration mode dominated by actin-independent blebbing protrusions [34]. The decrease in ATP consumption upon the switch in the migration mode could have suppressed the expected increase in lactate production in this experiment (Fig 2D). Whether the switch in the mode of migration is driven by changes in gene expression caused directly by HIF1 stabilization or by the metabolic changes in response to HIF1 stabilization remains a very interesting but yet unanswered question.

Another scenario wherein differing ATP requirements can underlie the observed metabolic heterogeneity is collective invasion by tumor cells. Leader cells, which are at the invading edge of the tumor cell pack and use ATP for actin-driven membrane protrusion, for maintaining

focal adhesion stability, and for remodeling the extracellular matrix, have a higher ATP requirement as compared to the trailing follower cells. To increase ATP production, leader cells must rely on the TCA cycle and oxidative phosphorylation which help drive a large flux through any pathway that consumes ATP (see inset in Fig 2A). Our model predicts that given the reliance of leader cells on the TCA cycle, they will likely proliferate at a rate lower than that of follower cells (which exhibit high lactate production) for a range of ATP consumption rates (between 10^{-2} and 10^{-1} on the horizontal axis in Fig 2A, for example). Such behavior was recently observed by Commander *et al.* [36] for the H1299 non-small cell lung cancer cell line —follower cells isolated from the cultures of this cell line exhibited higher lactate production and higher proliferation rates as compared to the leader cells from the same culture. Our model further predicts that under very high rates of ATP consumption when complete glucose oxidation via the TCA cycle (driven by high PDH1) is the preferred metabolic state, the phospholipids synthesis flux will increase upon the upregulation of GLUT1 (a glucose transporter) activity (Fig 2D). The observation that GLUT1 overexpression in leader cells can increase their proliferation rate [36] provides some preliminary evidence in support of this prediction.

The results reported in this section illustrate how our modeling framework can be used to explain the co-variation of such seemingly disparate phenotypes as cell proliferation and cell migration. Note that here we have focused on the phospholipids synthesis pathway as a representative example from the set of anabolic pathways that use glycolytic intermediates as substrates. The qualitative model predictions will remain unchanged for any other anabolic pathway of interest which relies upon glycolytic intermediates generated downstream from the enzyme PFK (for example, the serine synthesis pathway [37]) and are not limited by the availability of tumor redox capabilities.

Recently, Luengo *et al.* [30] have shown that aerobic glycolysis is also needed to drive fast tumor cell proliferation when NAD^+ availability is the limiting factor for anabolic processes including the synthesis of nucleotides, amino acids, and folate (see *Discussion* in Luengo *et al.* [30]). Further, the preference for aerobic glycolysis in such a scenario can be relieved by increasing the rate of ATP consumption by the tumor cells. To test if the present modeling framework can capture this behavior, we relaxed our assumption of a constant cytosolic NAD^+: NADH ratio and incorporated the glycerol-3-phosphate shuttle [28] into the model (see S1 Text). In agreement with the experimental observations of Luengo *et al.*, we observed that the cytosolic NAD^+: NADH ratio decreased with an increase in PDH activity (S1A Fig). This is accompanied by a decline in the NAD^+ use flux, a quantity which serves as a proxy for the rate of proliferation when NAD^+ availability is limiting (S1B Fig). Moreover, the model predicts that while the Warburg effect phenotype (high LDH, low PDH) can drive a high NAD^+ use flux when the rate of ATP consumption is low, cells must switch to a state with high PDH activity to drive fast proliferation at high ATP consumption rates (S1C Fig). This is an example of how the present model can easily be extended to other contexts, including those wherein the cell's redox capabilities (in the form of NAD^+ availability) rather than carbon substrate availability limit fast proliferation.

Distinct anaplerotic pathways can contribute towards de novo fatty acid synthesis

Fatty acids are a key biomolecular requirement for membrane synthesis, a necessity for cell division. While some tumor cells can take up fatty acids from the extracellular environment, others must synthesize the required fatty acids *de novo* [38]. A key substrate for fatty acid synthesis is acetyl-CoA, an intermediate of the TCA cycle, which is removed from the TCA cycle as citrate (Fig 3A). In the cytoplasm, the enzyme ACLY converts citrate back to acetyl-CoA.

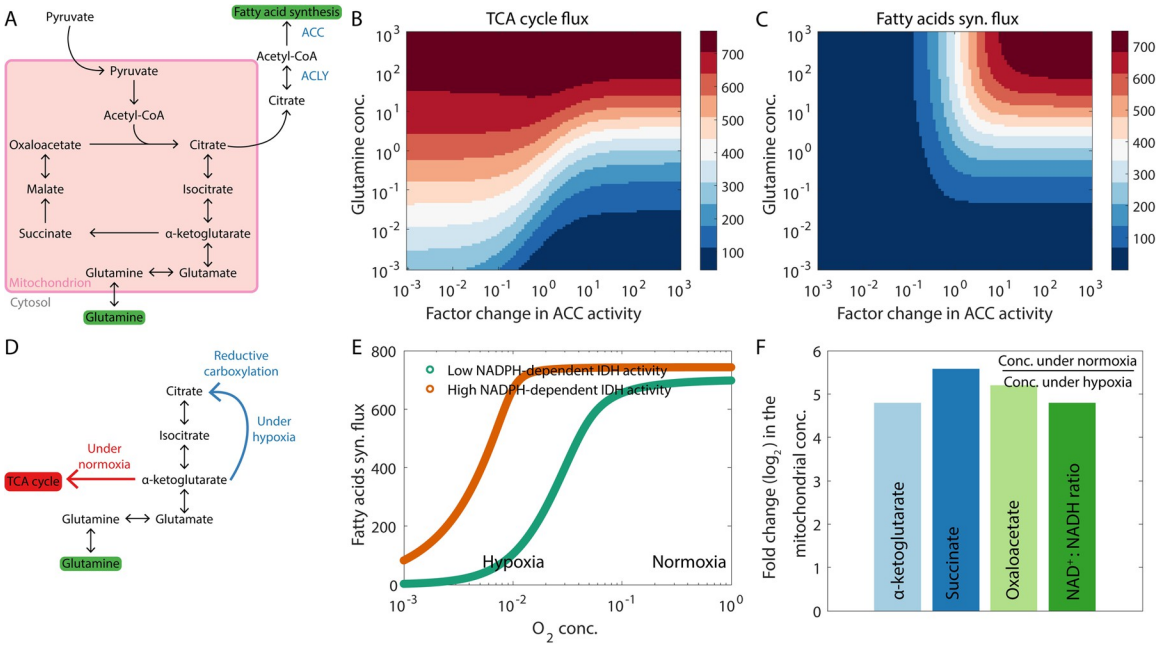

Fig 3. Glutamine is a key metabolite for anaplerosis during *de novo* fatty acid synthesis and can be utilized via different pathways under different conditions. (A) Reactions in the TCA cycle. The citrate removed from the TCA cycle for use as a substrate for fatty acid synthesis is replenished by the α-ketoglutarate generated from glutamine. (B) At high rates of *de novo* fatty acid synthesis (indicated by high ACC activity), our model predicts that the TCA cycle will shut down at low glutamine concentrations. Here, the flux through the enzyme α-ketoglutarate dehydrogenase is shown as the TCA cycle flux. (C) High glutamine availability can drive a large fatty acid synthesis flux. (D) Glutamine can be utilized for fatty acid synthesis via distinct pathways under normoxic and hypoxic conditions. (E) Under hypoxic conditions, glutamine can be utilized via the reductive carboxylation pathway (see panel D). High activity of NADPH-dependent IDH is essential for reductive carboxylation. (F) Ratio of the concentration of different TCA cycle intermediates under normoxic conditions to the concentration under hypoxic conditions. The panel also shows the ratio of the mitochondrial NAD^+:NADH ratios under the two conditions. Since the NADPH-dependent IDH pathway (active under hypoxic conditions) skips the TCA cycle reactions, activation of this pathway is accompanied by a decrease in the mitochondrial concentrations of multiple TCA cycle intermediates. Fluxes are in units of mM h^{-1} (millimolar per hour) and are shown at steady state.

https://doi.org/10.1371/journal.pcbi.1009841.g003

The enzyme ACC then converts acetyl-CoA to malonyl-CoA, a precursor for the synthesis of fatty acids [38]. To keep the sequence of reactions in the TCA cycle going, the intermediates must be replenished to compensate for the loss of citrate. The metabolic reactions that replenish the metabolites harvested from the TCA cycle for other cellular processes are called anaplerotic reactions [39]. Glutamine is a key biomolecule that can contribute towards anaplerosis during *de novo* fatty acid synthesis—glutamine can be converted to α-ketoglutarate which replenishes the carbon removed from the TCA cycle as citrate (Fig 3A). As shown in Fig 3B, when the fatty acid synthesis pathway is active (high ACC activity), our model predicts that the TCA cycle will shut down in the absence of glutamine unless there are other active pathways that can replenish the TCA cycle carbon lost as citrate. Sufficient glutamine availability is needed to drive a large flux through the fatty acid synthesis pathway (Fig 3C). Additionally, oxygen is essential for the oxidation of NADH via oxidative phosphorylation and the electron transport chain to keep the TCA cycle running. Therefore, the anaplerotic pathway described above can only function when oxygen is available (green curve in Fig 3E) since it involves all the reactions of the TCA cycle. Under hypoxic conditions, an alternate reaction pathway, mediated by NADPH-dependent IDH, may be activated to utilize glutamine for anaplerosis—reductive carboxylation of α-ketoglutarate to directly form citrate (Fig 3D and orange curve in Fig 3E). This model behavior is in agreement with the experimental observation that hypoxia can reprogram A549 lung cancer cells to rely on reductive glutamine metabolism, and

inhibition of NADPH-dependent IDH can suppress the proliferation of these cells [40]. The reductive carboxylation pathway is also relied upon by tumor cells with defective mitochondria to produce acetyl-CoA for fatty acid synthesis [41]. Continued fatty acid synthesis via reductive carboxylation will require the regeneration of NADPH. This may be achieved via the activity of the mitochondrial nicotinamide nucleotide transhydrogenase enzyme which uses NADH to convert the $NADP^+$ generated during reductive carboxylation back to NADPH [42]. Overall, our model shows that depending on the oxygen availability in different parts of the tumor microenvironment, proliferating cells can exhibit varying activity levels of different glutamine-driven anaplerotic pathways—oxidative glutamine metabolism under normoxic conditions and reductive glutamine metabolism under hypoxic conditions. Metabolic profiles of cells proliferating under normoxic and hypoxic conditions in a glutamine-dependent manner will therefore be different (Fig 3F). Note that ammonia is generated as a byproduct during glutamine utilization by tumor cells (specifically, during the conversion of glutamine to glutamate). Like lactate, ammonia has been known to build up in the tumor microenvironment, and is finally cleared by the liver via the urea cycle [43]. However, in some cases, tumor cells may be able to recycle ammonia for amino acid synthesis [44].

Under glutamine deprivation due to a lack of glutamine availability in the microenvironment or due to treatment with a drug that inhibits glutamine uptake, a glutamine-independent anaplerotic pathway will be needed for *de novo* fatty acid synthesis. Pyruvate carboxylase (PC) can drive one such pathway which involves the conversion of pyruvate to oxaloacetate (Fig 4A). As shown in Fig 4B, under conditions of glutamine deprivation, cells with high PC activity can drive fatty acid synthesis by generating both the precursors of citrate—oxaloacetate and acetyl-CoA—from glucose-derived pyruvate. Our model predicts that cells with low PC activity cannot synthesize fatty acids *de novo* under glutamine deprivation and are thus more likely to be sensitive to glutamine deprivation therapies. Consistent with our model prediction, MC-*38* mouse colon cancer cells, unable to upregulate PC activity, have been shown to be susceptible to glutamine blockade. We note in passing that in the same experimental setup, T cells showed increased PC activity upon glutamine deprivation and maintained a proliferative phenotype under glutamine blockade by using glucose for anaplerosis [45]. Glioblastoma cells have also been shown to switch to PC-driven anaplerosis under glutamine uptake inhibition [46]. In addition to glutamine deprivation, the nutrient environment can also trigger a switch to PC-driven anaplerosis and away from glutamine reliance [47]. Note that the PC-driven anaplerotic process short-circuits the TCA cycle (Fig 4A). Cells relying on this pathway will thus likely exhibit low TCA cycle flux and, consequently, a low oxygen consumption rate (Fig 4C) as compared to cells that rely on oxidative glutamine metabolism. Moreover, these cells will also exhibit low rates of lactate production as compared to glutamine-dependent cells since double the number of pyruvate molecules is now needed for citrate synthesis (Fig 4D), decreasing the availability of pyruvate for lactate production.

To determine if PC activity is indeed associated with low lactate production as per the above prediction, we used a short hairpin RNA (shPC) to downregulate the expression of PC in MDA-MB-468 breast cancer cells (Fig 4E). Arrows in Fig 4C and 4D indicate that downregulation of PC activity should be accompanied by a decline in the TCA cycle flux (and consequently, a decrease in the basal oxygen consumption rate (OCR)) and an increase in lactate production. This was confirmed by Seahorse analysis (Fig 4F) and NMR spectroscopy (Fig 4G), respectively. Interestingly, PC knockdown was also accompanied by an increase in the cellular glutamine concentration (Fig 4H) which would be needed to drive a large flux through the glutamine-dependent anaplerotic pathway. Increased glutamine uptake may thus compensate for decreased PC activity in MDA-MB-468 cells. Whether the increase in glutamine

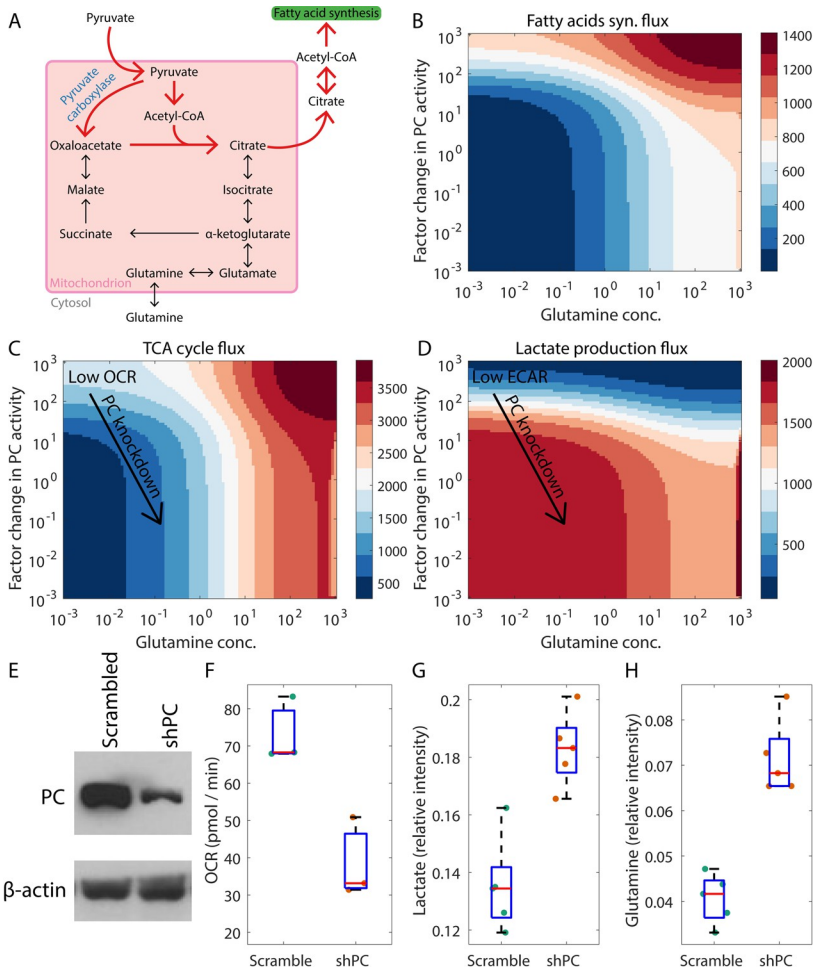

Fig 4. Pyruvate carboxylase (PC)-dependent anaplerosis under low glutamine concentrations. (A) Reactions involved in PC-dependent anaplerosis during fatty acid synthesis. (B) At low glutamine concentrations, high PC activity can help maintain a significant fatty acid synthesis flux. (C) and (D) When PC-dependent anaplerosis is the dominant anaplerotic pathway, cells carrying out *de novo* fatty acid synthesis will exhibit low TCA cycle flux and low oxidative phosphorylation (and consequently, low OCR) (C), and low lactate production (and consequently, low ECAR) (D). ECAR: extracellular acidification rate, which correlates positively with the rate of lactate excretion by cells. In panel C, the rate of conversion of TCA cycle-generated NADH to NAD^+ in an oxygen-dependent manner is shown as the TCA cycle flux. (E-G) Downregulating PC expression in MDA-MB-468 breast cancer cells decreases the oxygen consumption rate (OCR) and upregulates lactate production. (E) Western blot confirmed a decrease in the expression of the PC protein upon knockdown using PC shRNA compared to cells with control (Scrambled) shRNA. (F) Seahorse analysis shows decreased OCR in shPC cells (also, see arrow in panel C). NMR spectroscopy analysis shows increased lactate level (G) (also, see arrow in panel D) and increased glutamine level (H) in shPC cells. Fluxes are in units of mM h^{-1} (millimolar per hour) and are shown at steady state (B-D). Note that the arrow indicating PC knockdown in panels C and D is drawn diagonally (rather than vertically) downwards to reflect the overall effect of PC knockdown on tumor cell behavior: decrease in PC activity accompanied by an increase in glutamine uptake as seen in the experimental analysis (shown in panels E and H, respectively).

https://doi.org/10.1371/journal.pcbi.1009841.g004

uptake upon PC knockdown is driven purely by metabolic feedback or by some gene regulatory mechanism remains to be determined.

Finally, we examined the model behavior under glucose deprivation and sufficient glutamine availability. As shown in Figs 1A and 5C, cells are unlikely to be able to proliferate under such conditions [48]. This is because key anabolic processes that use glycolytic intermediates as substrates, such as the ribose synthesis and the phospholipids synthesis pathways, will likely shut down when glucose is unavailable. However, cells can survive in such a scenario provided

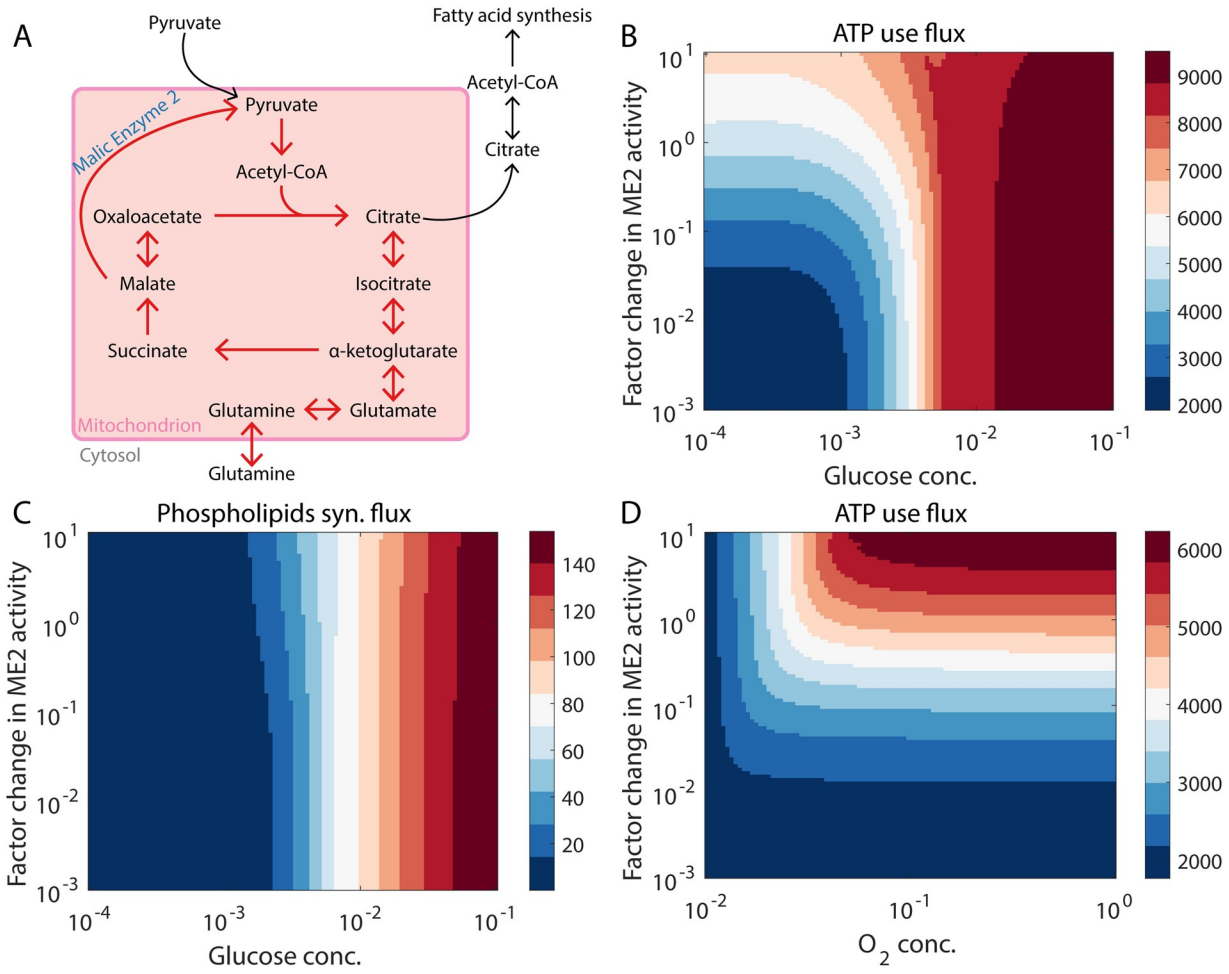

Fig 5. Glutamine can drive the TCA cycle in the absence of glucose. (A) Reactions involved in the glutamine-driven TCA cycle when glucose concentration is low. (B) Under low glucose concentrations, malic enzyme 2 (ME2) activity must be upregulated to maintain a significant ATP production rate. (C) In the absence of glucose, the phospholipids synthesis flux remains low, irrespective of the ME2 activity. Thus, cells are unlikely to proliferate under low glucose concentrations [48]. (D) Oxygen is essential for maintaining a significant flux through pathways that consume ATP when glutamine is available, but the glucose concentration is low. Fluxes are in units of mM h^{-1} (millimolar per hour) and are shown at steady state.

https://doi.org/10.1371/journal.pcbi.1009841.g005

sufficient ATP is available to keep the basal cellular processes going. ATP can be generated in the absence of glucose by utilizing glutamine to drive the TCA cycle (Fig 5A) as has been shown for the P493 Burkitt lymphoma cell line [49]. The enzyme ME2 (malic enzyme 2), which converts malate directly to pyruvate, can help drive a glutamine-dependent TCA cycle. Cells with high ME2 activity can thus survive glucose deprivation by using glutamine to generate ATP (Fig 5B). In agreement with our model prediction, inhibition of both mitochondrial pyruvate import and the enzyme glutamate dehydrogenase (a key enzyme for generating α-ketoglutarate from glutamine) has been shown to be cytotoxic in glioblastoma cells as compared to only inhibiting mitochondrial pyruvate import [50]. Note that ATP synthesis from glutamine in a glucose-independent manner is oxygen-dependent (Fig 5D)—the process involves an operational TCA cycle which generates NADH, and the conversion of glutamate to α-ketoglutarate generates an additional NADH molecule. Oxygen must be available for the oxidation of NADH to NAD^+ via the electron transport chain, a process that generates ATP. Under hypoxic conditions, NADH will accumulate and shut down not only the TCA cycle but

also the entry of glutamine into the TCA cycle (Fig 5D). Cells in hypoxic niches are thus less likely to survive glucose deprivation as compared to cells in normoxic niches. We do note that some tumor cells have been shown to proliferate under glucose deprivation by synthesizing glycolytic intermediates from non-glucose substrates including from glutamine via the mitochondrial isoform of the PEPCK enzyme [51].

Interplay between metabolic plasticity and drug response in melanoma

Paudel *et al.* [52] observed that single-cell-derived subclones of the SKMEL5 melanoma cell line, which carries a BRAF mutation, exhibit heterogeneity in their short-term response to the BRAF inhibitor PLX4720 (Fig 6A; also see *Figs 2A and 3A* in Paudel *et al.* [52]). Since BRAF signaling inhibition can suppress glutamine uptake by downregulating MYC [55,56], cells proliferating under PLX4720 treatment may resort to glutamine-independent anaplerotic pathways such as the PC-mediated pathway described above. We analyzed the gene expression profiles of the SKMEL5 subclones (reported by Jia *et al.* [53]) and observed that the expression of PC is upregulated in the SC10 subclone upon PLX4720 treatment (Fig 6B). Surprisingly, among the three subclones for which gene expression data is available, only SC10 showed population expansion in the short-term (<150 hours) after PLX4720 treatment (Fig 6A). While subclone SC07 population is stationary, subclone SC01 exhibits population regression upon PLX4720 treatment. Both these subclones did not exhibit increased PC expression upon drug treatment (Fig 6B). Our modeling framework predicts that if SC10 cells are reliant on PC for anaplerosis under PLX4720 treatment as PC upregulation upon drug treatment would suggest, they must exhibit a low oxygen consumption rate (low OCR) and a low extracellular acidification rate due to low lactate production (low ECAR) (Fig 4C). Indeed, upon PLX4720 treatment, SC10 cells have been shown to switch to a metabolic state with low OCR and low ECAR (see *Fig 2D* in Jia *et al.* [53]). We further analyzed the gene expression profiles of melanoma tissue samples obtained from patients before and after treatment with a BRAF signaling inhibitor [54] (Gene Expression Omnibus [57] accession GSE75299). Out of the six patient samples, four exhibited upregulation of PC upon drug-induced BRAF signaling inhibition (Fig 6C). This is accompanied by the downregulation of MYC, a well-known target of BRAF signaling. Thus, our analysis suggests, albeit preliminarily, that PC-mediated anaplerosis may play a key role in the response of melanoma cells to treatment with BRAF signaling inhibitors, at least at short time scales. One immediate consequence of this observation is the suggestion that co-treatment with inhibitors of BRAF and PC could be a promising anti-melanoma therapy.

Discussion

Multiple studies have shown that tumor cells within the primary tumor and those at different stages of metastatic progression exhibit widespread heterogeneity in their metabolic profiles [4,5]. The metabolic phenotype can also co-vary with other functional attributes such as morphology [58], migratory phenotype [35,36], and stemness [59]. Here, using a detailed mechanistic model of some of the key metabolic pathways in tumor cells, we show that variation in ATP usage can be a key driver of the metabolic heterogeneity exhibited by tumor cells. Differences in the availability of nutrients and in the ability of tumor cells to take up these nutrients can further contribute towards the diversity of metabolic profiles. Our modeling framework can predict the metabolic profiles that tumor cells will exhibit under various external interventions and in different environmental contexts. By using a mechanistic modeling approach, our study avoids the difficulties associated with choosing an appropriate objective function and appropriate constraints that plague constraint-based models. Further, our modeling approach captures the effect of feedback loops in metabolic pathways, and we show that these are crucial

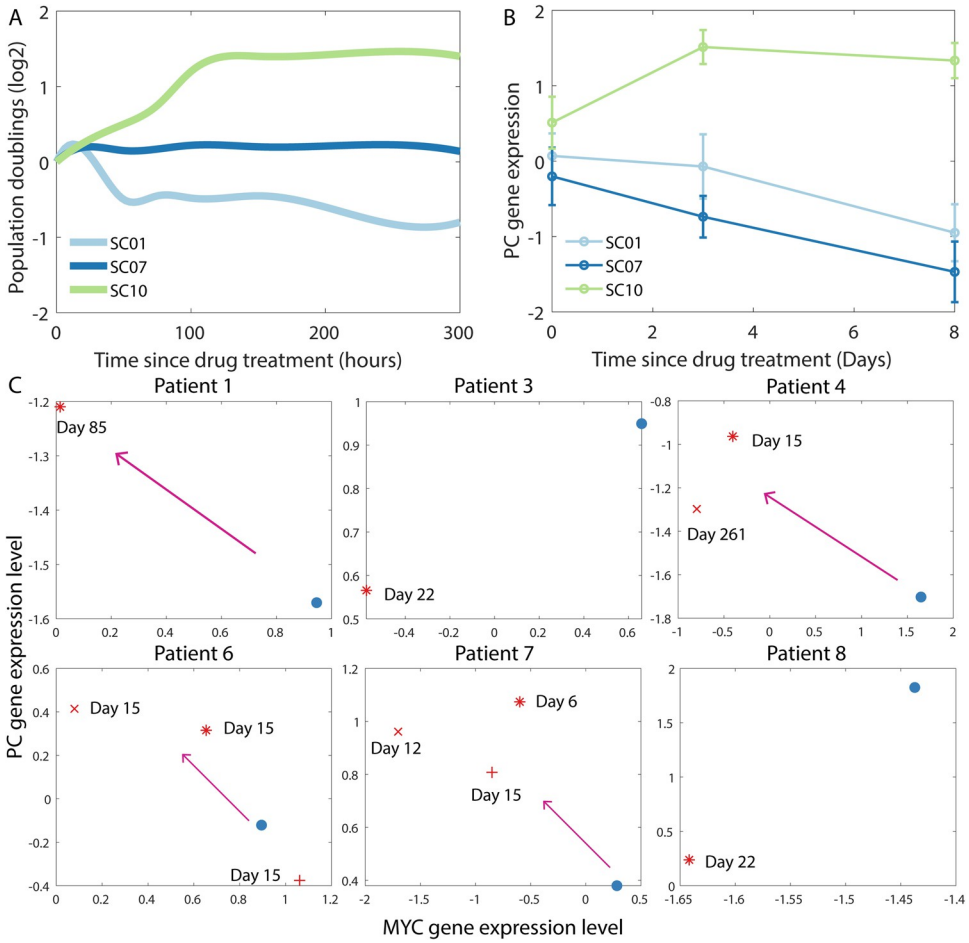

Fig 6. Pyruvate carboxylase (PC) expression levels are altered in melanoma cells in response to BRAF signaling inhibitors. (A) Representative depiction of the response of three different subclones of the SKMEL5 melanoma cell line to treatment with PLX4720, a mutant BRAF inhibitor, as reported by Paudel *et al.* [52] (see *Fig 3A* therein). (B) RNA expression levels of the PC gene (Z-score calculated after log*2* normalization) in the three subclones in (A) at *3* days and *8* days post-treatment with PLX4720. The gene expression data was obtained from Jia *et al.* [53]. The error bars indicate the standard deviation. (C) RNA expression levels of MYC and PC genes (Z-score calculated after log*2* normalization) in tumor samples obtained from melanoma patients. In each panel, the blue dot indicates the expression levels before treatment. The different red markers in each panel indicate the expression levels in samples obtained at different time points after treatment with BRAF signaling inhibitors. The gene expression data was downloaded from the Gene Expression Omnibus databse (accession GSE75299). See Song *et al.* [54] for details regarding the patient samples and the BRAF signaling inhibitor administered in each case. In panels C and D, the Z-scores were calculated as $Z_i^{PC} = \frac{E_i^{PC} - \mu^{PC}}{\sigma^{PC}}$ where E_i^{PC} is the PC expression level in the i^{th} sample while μ^{PC} and σ^{PC} are the mean and standard deviation of the PC expression levels in the dataset, respectively.

https://doi.org/10.1371/journal.pcbi.1009841.g006

to understanding the metabolic heterogeneity exhibited by tumor cells. Exploring the possible set of metabolic profiles that can be obtained by varying the reaction velocities in the model instead of fitting the model parameters to a set of experimental observations concerning a specific cell line allowed us to develop a broad framework to analyze diverse tumor metabolic profiles instead of making predictions pertaining only to a given experimental setup. While the framework in the present study does not include all the metabolic pathways active in tumor cells as is usually the case for genome-scale metabolic models [6], the predictions from our framework are far more interpretable and propose key principles that underly the metabolic profiles seen across tumor types. These principles could hold the key to identifying metabolic targets for anti-cancer therapy [5].

The model described in the present study can also be used to analyze the metabolic behaviors of rapidly proliferating normal, non-tumoral mammalian cells. These cells also consume glucose and glutamine as the key nutrients during proliferation. Rapidly proliferating stem cells [60] and activated T cells [61] have been shown to exhibit the Warburg effect. In the present study, we have identified the possible metabolic behaviors that cells can adopt to sustain fast proliferation under varying nutrient and oxygen availabilities. Gene dysregulations driving such behaviors are common in tumor cells. Tumor cells across cancer types have been shown to upregulate GLUT1 which, as shown in Figs 1B and 2E, is needed to drive large anabolic fluxes through pathways that use glycolytic intermediates as substrates [62]. Multiple oncogenes are involved in reprogramming glutamine metabolism to drive fast proliferation in tumor cells, including MYC which is known to upregulate the glutamine transporter SLC1A5 to increase the glutamine uptake, and the enzymes GLS1 / 2 which convert glutamine to glutamate [63]. Tumor cells have also been shown to upregulate the expression of the NADPH-dependent isoform of IDH which, as shown in Fig 3E, is needed for glutamine-driven anaplerosis under hypoxic conditions [64]. Overexpression of pyruvate carboxylase, needed for fatty acid synthesis under glutamine deprivation as shown in Fig 4B, has been associated with tumor aggressiveness [65]. Finally, ME2, required for ATP production and tumor cell survival under glucose unavailability (as shown in Fig 5B), is also overexpressed in multiple tumors [66] and its deletion has been shown to decrease ATP production and induce cell death [67]. The metabolic pathways that can drive fast proliferation across contexts are available in normal cells as well. However, in these cells, the activation of these pathways is tightly controlled to prevent uncontrolled proliferation. In tumors, oncogenic mutations and processes can hijack these pathways to drive aberrant activation of the fast proliferation phenotype.

Our model predicts that in order to drive large fluxes through anabolic pathways that are crucial to fast proliferation, the cytosolic ATP concentration must be kept below a threshold to maintain the activity of PFK, a key enzyme in the glucose uptake pathway. While increased proliferation rate can raise the ATP consumption rate, the increase may not be enough to relieve the inhibition of PFK by ATP. This can explain why tumor cells, across cancer types, often prefer aerobic glycolysis over oxidative phosphorylation—the ATP yield per glucose molecule from aerobic glycolysis is less than one-tenth of the yield from oxidative phosphorylation [32]. That the inhibition of PFK by high levels of ATP can drive aerobic glycolysis in tumor cells was first postulated by Scholnick *et al.* [68] nearly half a century ago. An important corollary that follows from this prediction is that the preference of tumor cells for aerobic glycolysis versus oxidative phosphorylation can be modulated by the rate of ATP consumption in these cells. We have built upon this corollary to describe how the metabolic state of tumor cells can depend on their migratory phenotype [35,36]. The framework can also be helpful in understanding other behaviors exhibited by tumor and other fast proliferating cells. For example, the PI3K / Akt signaling pathway, which is activated in response to extracellular growth factors in normal, non-cancerous cells [69], transcriptionally upregulates ENTPD5. ENTPD5 promotes proper protein glycosylation and protein folding via a cycle of reactions that convert ATP to ADP [70,71]. Our model would predict that the resulting increase in ATP consumption will relieve the inhibition of PFK by ATP, thereby increasing the flux through anabolic pathways such as the phospholipids synthesis pathway, facilitating fast proliferation. Knockdown of ENTPD5 has indeed been shown to inhibit cell growth in PTEN-null mouse embryonic fibroblasts by Fang *et al.* [70] who also reported a decrease in PFK enzymatic activity upon ENTPD5 knockdown. The increased glycolytic flux from upregulated ATP consumption can also account for the observed upregulation of ATPases such as the Na^+ / K^+ pump in tumor cells [72–74]. The idea that the operation of the Na^+ / K^+ pump can alter the rate of glycolysis was also proposed by Scholnick *et al.* [68]. Note that the model of tumor metabolism

described here does not incorporate ATP production from other metabolic pathways including from the β-oxidation of fatty acids. Inclusion of β-oxidation in the present model could shed light on the interplay between fatty acid metabolism and other cell behaviors including proliferation rates, and further unravel the context-dependence of fast proliferation rates on glycolytic flux.

Luengo *et al.* [30] have proposed that increased NAD^+ demand for oxidation as compared to the ATP demand during cell proliferation can drive a preference for aerobic glycolysis in multiple cell lines. In such a scenario, high ATP concentration and low ADP availability, resulting from low ATP usage, inhibits the regeneration of NAD^+ from the NADH produced during the TCA cycle. The limited NAD^+ availability limits cell proliferation. In the modeling framework described in the present study, high ATP concentration resulting from low ATP usage also drives a preference for aerobic glycolysis. However, in our framework, the NAD^+ concentration is not limiting. Rather, it is the anabolic fluxes, such as the flux through the phospholipids synthesis pathway, that become limiting due to the inhibition of PFK by ATP. The focus on increased anabolic fluxes required for cell division allows us to capture the increased glucose uptake and lactate production in tumor cells. Limited NAD^+ availability cannot account for the increased lactate production since uptake of carbon as glucose and its excretion as lactate is redox neutral overall. The two ideas, one described by Luengo *et al.* [30] and the other proposed in the present study, may be applicable in different scenarios depending on whether NAD^+ is limiting or not.

Tumor cells, across cancer types, can rely on different growth signaling pathways to drive continued cell proliferation [75,76]. Different growth signaling pathways often activate distinct pathways to drive the same cellular process. For example, in prostate cancer cells, androgen-receptor mediated signaling promotes the uptake of fatty acids from the extracellular environment while PI3K / Akt signaling drives *de novo* fatty acid synthesis [38]. In the case of breast cancer, receptor-positive breast cancer cells rely primarily on *de novo* fatty acid synthesis while basal-like, receptor-negative breast cancer cells take up fatty acids from the extracellular environment [77]. The present modeling framework can provide useful insights into the metabolic profiles of cancer cells reliant on different growth signaling pathways. Our model predicts that tumor cells that synthesize fatty acids *de novo* must increase their glutamine uptake or upregulate the expression of the enzyme PC. While cells taking up glutamine will maintain high lactate production, lactate production will be down-regulated in cells upregulating PC activity. In contrast, tumor cells that can take up fatty acids can rely on these both for ATP generation (via β-oxidation) and for anabolic processes. These cells will thus likely have both low glutamine uptake and low glucose uptake. Prostate cancer cells treated with an inhibitor of androgen receptor signaling such as enzalutamide can develop resistance by activating the PI3K / Akt signaling pathway, thereby turning on *de novo* fatty acid synthesis [78]. Our modeling framework predicts that the emergence of enzalutamide resistance must be accompanied by a change in the metabolic profile of tumor cells including an increase in glucose uptake. A recent study has shown that the activities of signaling pathways that regulate cell metabolism, including the p38 pathway, are indeed altered by enzalutamide treatment in prostate cancer cells [79].

Multiple studies have shown a tight coupling between cell-type switching and change in the metabolic state of cells, especially in the context of epithelial-mesenchymal plasticity. Bhattacharya *et al.* [80] showed that neural crest cells in a chicken embryo activate aerobic glycolysis at the onset of cell migration and that an increase in glycolytic flux is essential for driving an epithelial to mesenchymal transition. Luo *et al.* [58] have shown that inhibition of glucose uptake via treatment with *2*-deoxyglucose leads to an increase in reactive oxygen species (ROS) concentration, causing mesenchymal breast cancer stem cells to switch to a more

epithelial state (but not to a fully epithelial state). Our modeling framework suggests that inhibition of glucose uptake will lead to increased reliance on glutamine for ATP production (Fig 5A and 5B). Apart from playing a key role in anaplerosis and in glucose-independent ATP production, glutamine also drives an anti-oxidant response via the glutathione pathway [81]. Treatment with *2*-deoxyglucose could thus decrease the availability of glutamine for the anti-oxidant response. The consequent increase in ROS concentration can upregulate NRF2 which has been shown to stabilize a hybrid epithelial-mesenchymal state [82]. Further, given the low availability of glutamine for the anti-oxidant pathway, epithelial cells would be more susceptible to thioredoxin suppression [58] (thioredoxin mediates a glutamine-independent anti-oxidant response). Incorporating ROS generation and anti-oxidant pathways into the present modeling framework could thus help further our understanding of metabolic dependence in cell-type switching.

Finally, the present model can be extended to develop a population-level framework to analyze the interaction between tumor cells exhibiting different metabolic phenotypes. For example, tumor cells exhibiting glycolysis can cooperate with non-glycolytic tumor cells by excreting lactate which can be taken up by the neighboring cells and metabolized via the TCA cycle [83]. The lactate excreted by glycolytic tumor cells has also been shown to support the metabolic needs of tumor-promoting regulatory T cells, and suppression of the lactate transporter MCT1 in regulatory T cells has been shown to synergize with anti-PD-1 therapy in a mouse model of melanoma [84]. Moreover, tumor cells and immune cells compete for nutrients in the tumor microenvironment and tilting the competition towards tumor-suppressive immune cells can prove to be an effective anti-tumor strategy [45,85]. A population-level extension of the present framework could prove invaluable in developing strategies to modulate the metabolic interplay in the tumor microenvironment to a tumor-suppressive state.

Materials and methods

Cell culture and knockdown of pyruvate carboxylase

MDA-MB-468 breast cancer cells were maintained in DMEM cell culture medium supplemented with *5*% FBS, *100* units / ml penicillin, and *100* μg / ml streptomycin. The cell line was authenticated using short tandem repeat profiling by the MD Anderson Cancer Center Cytogenetics and Cell Authentication Core. pGIPZ lentivirus shRNA for pyruvate carboxylase (PC) was purchased from the Cell-Based Assay Screening Service (C-BASS) Core at Baylor College of Medicine. The lentivirus with scrambled (control) or PC-targeting shRNA was infected using the standard protocol [86]. Knockdown efficiency was validated by western blot analysis using specific antibodies.

Cell respiratory assay

Oxygen consumption rate (OCR) was measured using the XFp extracellular flux analyzer (Seahorse Biosciences) as previously described [86] with a minor modification. Cell Mito Stress kit (Seahorse Biosciences) was used for the assay and basal OCR was calculated by Report Generator Version 4.03 (Seahorse Biosciences).

High-resolution Nuclear Magnetic Resonance (NMR) Spectroscopy

Metabolites were extracted from cell pellets using *3* mL *2:1* methanol-water solvent and *0.5* ml of lysing beads (Lysing Matrix D from MP Biomedicals, LLC). The mixture was vortexed and freeze-thawed three times to extract the metabolites. This was followed by centrifugation at *4,000* RPM for *10* minutes to remove debris, and rotary evaporation and overnight

lyophilization to remove residual solvent. The samples were prepared for NMR spectroscopy by dissolving the lyophilized sample in *800* μL of $^{2}H_2O$ following the centrifugation at *10,000* RPM for *5* minutes to remove any debris that remained. Finally, *600* μL of the sample, with the addition of *40* μL of *8* mM NMR reference compound *2, 2*-dimethyl-*2*-silapentane-*5*-sulfonate (DSS), was used for NMR data acquisition. Final concentration of DSS in the sample was *0.5* mM. The standard one dimensional ^{1}H spectrum with water suppression during relaxation time was used to acquire the data. All *1*D ^{1}H spectra were acquired with *32*K time domain points, *2* seconds acquisition time, *256* transients, *64* receiver gain, *16* ppm spectral width, and *6* second relaxation delay on a Bruker NMR spectrometer (Bruker Biospin MRI GmbH, Ettlingen, Germany) operating at *500* MHz proton resonance frequency attached with cryogenically cooled triple resonance (^{1}H, ^{13}C, ^{15}N) prodigy BBO probe [87]. The data was processed using Topspin 3.1 and resonances were identified using Chenomx NMR suite 7.0 (Chenomx Inc., Edmonton, Canada) and the human metabolic database (HMDB) [88].

Supporting information

S1 Text. Detailed description of the mathematical model of tumor metabolism presented in the study, along with the assumptions underlying model construction.
(DOCX)

S1 Fig. Behavior of an extended model incorporating the glycerol-3-phosphate shuttle and dynamics of the cytosolic NAD^+: NADH ratio. (A) The cytoplasmic NAD^+: NADH ratio decreases with an increase in PDH activity. (B) The NAD^+ use flux, which determines the proliferation rate when NAD^+ is the limiting factor to fast proliferation, decreases with an increase in PDH activity. Note that the Warburg effect phenotype (high LDH, low PDH in the absence of oxygen deprivation) is characterized by a high NAD^+ use flux and can thus drive fast proliferation. (C) The regime that maximizes the NAD^+ use flux depends on the rate of cellular ATP use. The behavior in panel C is similar to the one shown in Fig 2A: while high LDH, low PDH activity can drive fast proliferation at low ATP consumption rates, high PDH activity is needed to maintain fast proliferation under high ATP use.
(TIF)

S2 Fig. Flux corresponding to the export of excess α-ketoglutarate generated from glutamine during oxidative glutamine metabolism (low NADPH-dependent IDH activity) compared with the flux during reductive glutamine metabolism (high NADPH-dependent IDH activity). Simulation conditions are the same as shown in Fig 3E in the main text.
(TIF)

Author Contributions

Conceptualization: Shubham Tripathi, Herbert Levine.

Investigation: Shubham Tripathi, Jun Hyoung Park, Shivanand Pudakalakatti, Pratip K. Bhattacharya.

Methodology: Shubham Tripathi, Jun Hyoung Park.

Supervision: Benny Abraham Kaipparettu, Herbert Levine.

Writing – original draft: Shubham Tripathi.

Writing – review & editing: Shubham Tripathi, Jun Hyoung Park, Benny Abraham Kaipparettu, Herbert Levine.

References

1. Hanahan D, Weinberg RA. Hallmarks of Cancer: The Next Generation. Cell. 2011; 144: 646–674. https://doi.org/10.1016/j.cell.2011.02.013 PMID: 21376230
2. Martinez-Outschoorn UE, Peiris-Pagés M, Pestell RG, Sotgia F, Lisanti MP. Cancer metabolism: a therapeutic perspective. Nat Rev Clin Oncol. 2017; 14: 11–31. https://doi.org/10.1038/nrclinonc.2016.60 PMID: 27141887
3. Warburg O, Posener K, Negelein E. Üeber den Stoffwechsel der Tumoren. Biochem Z. 1924; 152: 319–344. https://doi.org/10.1007/BF01726240
4. Lehuédé C, Dupuy F, Rabinovitch R, Jones RG, Siegel PM. Metabolic Plasticity as a Determinant of Tumor Growth and Metastasis. Cancer Res. 2016; 76: 5201–5208. https://doi.org/10.1158/0008-5472.CAN-16-0266 PMID: 27587539
5. Faubert B, Solmonson A, DeBerardinis RJ. Metabolic reprogramming and cancer progression. Science. 2020; 368: eaaw5473. https://doi.org/10.1126/science.aaw5473 PMID: 32273439
6. Yizhak K, Chaneton B, Gottlieb E, Ruppin E. Modeling cancer metabolism on a genome scale. Molecular Systems Biology. 2015; 11: 817. https://doi.org/10.15252/msb.20145307 PMID: 26130389
7. Vazquez A, Liu J, Zhou Y, Oltvai ZN. Catabolic efficiency of aerobic glycolysis: The Warburg effect revisited. BMC Syst Biol. 2010; 4: 58. https://doi.org/10.1186/1752-0509-4-58 PMID: 20459610
8. Shlomi T, Benyamini T, Gottlieb E, Sharan R, Ruppin E. Genome-Scale Metabolic Modeling Elucidates the Role of Proliferative Adaptation in Causing the Warburg Effect. PLoS Comput Biol. 2011; 7: e1002018. https://doi.org/10.1371/journal.pcbi.1002018 PMID: 21423717
9. Folger O, Jerby L, Frezza C, Gottlieb E, Ruppin E, Shlomi T. Predicting selective drug targets in cancer through metabolic networks. Molecular Systems Biology. 2011; 7: 501. https://doi.org/10.1038/msb.2011.35 PMID: 21694718
10. Asgari Y, Salehzadeh-Yazdi A, Schreiber F, Masoudi-Nejad A. Controllability in Cancer Metabolic Networks According to Drug Targets as Driver Nodes. PLOS ONE. 2013; 8: e79397. https://doi.org/10.1371/journal.pone.0079397 PMID: 24282504
11. Facchetti G, Zampieri M, Altafini C. Predicting and characterizing selective multiple drug treatments for metabolic diseases and cancer. BMC Syst Biol. 2012; 6: 115. https://doi.org/10.1186/1752-0509-6-115 PMID: 22932283
12. Agren R, Mardinoglu A, Asplund A, Kampf C, Uhlen M, Nielsen J. Identification of anticancer drugs for hepatocellular carcinoma through personalized genome-scale metabolic modeling. Molecular Systems Biology. 2014; 10: 721. https://doi.org/10.1002/msb.145122 PMID: 24646661
13. Nam H, Campodonico M, Bordbar A, Hyduke DR, Kim S, Zielinski DC, et al. A Systems Approach to Predict Oncometabolites via Context-Specific Genome-Scale Metabolic Networks. PLOS Computational Biology. 2014; 10: e1003837. https://doi.org/10.1371/journal.pcbi.1003837 PMID: 25232952
14. Gatto F, Nookaew I, Nielsen J. Chromosome 3p loss of heterozygosity is associated with a unique metabolic network in clear cell renal carcinoma. PNAS. 2014; 111: E866–E875. https://doi.org/10.1073/pnas.1319196111 PMID: 24550497
15. Goldstein I, Yizhak K, Madar S, Goldfinger N, Ruppin E, Rotter V. p53 promotes the expression of gluconeogenesis-related genes and enhances hepatic glucose production. Cancer & Metabolism. 2013; 1: 9. https://doi.org/10.1186/2049-3002-1-9 PMID: 24280180
16. Roy M, Finley SD. Computational Model Predicts the Effects of Targeting Cellular Metabolism in Pancreatic Cancer. Front Physiol. 2017;8. https://doi.org/10.3389/fphys.2017.00008 PMID: 28167916
17. Jia D, Lu M, Jung KH, Park JH, Yu L, Onuchic JN, et al. Elucidating cancer metabolic plasticity by coupling gene regulation with metabolic pathways. Proc Natl Acad Sci USA. 2019; 116: 3909–3918. https://doi.org/10.1073/pnas.1816391116 PMID: 30733294
18. Orth JD, Thiele I, Palsson BØ. What is flux balance analysis? Nature Biotechnology. 2010; 28: 245–248. https://doi.org/10.1038/nbt.1614 PMID: 20212490
19. Huang B, Lu M, Jia D, Ben-Jacob E, Levine H, Onuchic JN. Interrogating the topological robustness of gene regulatory circuits by randomization. PLoS Comput Biol. 2017; 13: e1005456. https://doi.org/10.1371/journal.pcbi.1005456 PMID: 28362798
20. Huang B, Lu M, Galbraith M, Levine H, Onuchic JN, Jia D. Decoding the mechanisms underlying cell-fate decision-making during stem cell differentiation by random circuit perturbation. Journal of The Royal Society Interface. 2020; 17: 20200500. https://doi.org/10.1098/rsif.2020.0500 PMID: 32781932
21. Lunt SY, Vander Heiden MG. Aerobic Glycolysis: Meeting the Metabolic Requirements of Cell Proliferation. Annu Rev Cell Dev Bio. 2011; 27: 441–464. https://doi.org/10.1146/annurev-cellbio-092910-154237 PMID: 21985671

22. Mulukutla BC, Yongky A, Daoutidis P, Hu W-S. Bistability in Glycolysis Pathway as a Physiological Switch in Energy Metabolism. PLOS ONE. 2014; 9: e98756. https://doi.org/10.1371/journal.pone.0098756 PMID: 24911170

23. Wu F, Yang F, Vinnakota KC, Beard DA. Computer Modeling of Mitochondrial Tricarboxylic Acid Cycle, Oxidative Phosphorylation, Metabolite Transport, and Electrophysiology. J Biol Chem. 2007; 282: 24525–24537. https://doi.org/10.1074/jbc.M701024200 PMID: 17591785

24. Engel PC, Dalziel K. Kinetic studies of glutamate dehydrogenase. The reductive amination of 2-oxoglutarate. Biochem J. 1970; 118: 409–419. https://doi.org/10.1042/bj1180409 PMID: 4394334

25. Barden RE, Fung CH, Utter MF, Scrutton MC. Pyruvate carboxylase from chicken liver. Steady state kinetic studies indicate a "two-site" ping-pong mechanism. J Biol Chem. 1972; 247: 1323–1333. https://doi.org/10.1016/S0021-9258(19)45648-2 PMID: 5010071

26. Mallick S, Harris BG, Cook PF. Kinetic mechanism of NAD:malic enzyme from Ascaris suum in the direction of reductive carboxylation. J Biol Chem. 1991; 266: 2732–2738. https://doi.org/10.1016/S0021-9258(18)49906-1 PMID: 1993653

27. Nazaret C, Heiske M, Thurley K, Mazat J-P. Mitochondrial energetic metabolism: A simplified model of TCA cycle with ATP production. J Theor Biol. 2009; 258: 455–464. https://doi.org/10.1016/j.jtbi.2008.09.037 PMID: 19007794

28. Mráček T, Drahota Z, Houštěk J. The function and the role of the mitochondrial glycerol-3-phosphate dehydrogenase in mammalian tissues. Biochim Biophys Acta Bioenerg. 2013; 1827: 401–410. https://doi.org/10.1016/j.bbabio.2012.11.014 PMID: 23220394

29. Borst P. The malate–aspartate shuttle (Borst cycle): How it started and developed into a major metabolic pathway. IUBMB Life. 2020; 72: 2241–2259. https://doi.org/10.1002/iub.2367 PMID: 32916028

30. Luengo A, Li Z, Gui DY, Sullivan LB, Zagorulya M, Do BT, et al. Increased demand for NAD+ relative to ATP drives aerobic glycolysis. bioRxiv. 2020; 2020.06.08.140558. https://doi.org/10.1016/j.molcel.2020.12.012 PMID: 33382985

31. Berg JM, Tymoczko JL, Stryer L. Enzymes: Basic Concepts and Kinetics. 5th ed. Biochemistry. 5th ed. New York: W. H. Freeman and Company; 2002. pp. 189–226.

32. Nelson DL, Cox MM. The Citric Acid Cycle. 4th ed. Lehninger Principles of Biochemistry. 4th ed. New York: W. H. Freeman and Company; 2005. pp. 601–630.

33. Nelson DL, Cox MM. Glycolysis, Gluconeogenesis, and the Pentose Phosphate Pathway. 4th ed. Lehninger Principles of Biochemistry. 4th ed. New York: W. H. Freeman and Company; 2005. pp. 521–559.

34. Li Y, Yao L, Mori Y, Sun SX. On the energy efficiency of cell migration in diverse physical environments. Proc Natl Acad Sci USA. 2019; 116: 23894–23900. https://doi.org/10.1073/pnas.1907625116 PMID: 31719206

35. Boekhorst V te, Jiang L, Mähler M, Meerlo M, Dunkel G, Durst FC, et al. Calpain-2 regulates hypoxia/HIF-induced amoeboid reprogramming and metastasis. bioRxiv. 2020; 2020.01.06.892497. https://doi.org/10.1101/2020.01.06.892497

36. Commander R, Wei C, Sharma A, Mouw JK, Burton LJ, Summerbell E, et al. Subpopulation targeting of pyruvate dehydrogenase and GLUT1 decouples metabolic heterogeneity during collective cancer cell invasion. Nat Commun. 2020; 11: 1533. https://doi.org/10.1038/s41467-020-15219-7 PMID: 32210228

37. Baksh SC, Todorova PK, Gur-Cohen S, Hurwitz B, Ge Y, Novak JSS, et al. Extracellular serine controls epidermal stem cell fate and tumour initiation. Nat Cell Biol. 2020; 22: 779–790. https://doi.org/10.1038/s41556-020-0525-9 PMID: 32451440

38. Koundouros N, Poulogiannis G. Reprogramming of fatty acid metabolism in cancer. Br J Cancer. 2020; 122: 4–22. https://doi.org/10.1038/s41416-019-0650-z PMID: 31819192

39. Brunengraber H, Roe CR. Anaplerotic molecules: current and future. J Inherit Metab Dis. 2006; 29: 327–331. https://doi.org/10.1007/s10545-006-0320-1 PMID: 16763895

40. Metallo CM, Gameiro PA, Bell EL, Mattaini KR, Yang J, Hiller K, et al. Reductive glutamine metabolism by IDH1 mediates lipogenesis under hypoxia. Nature. 2012; 481: 380–384. https://doi.org/10.1038/nature10602 PMID: 22101433

41. Mullen AR, Wheaton WW, Jin ES, Chen P-H, Sullivan LB, Cheng T, et al. Reductive carboxylation supports growth in tumour cells with defective mitochondria. Nature. 2012; 481: 385–388. https://doi.org/10.1038/nature10642 PMID: 22101431

42. Mullen AR, Hu Z, Shi X, Jiang L, Boroughs LK, Kovacs Z, et al. Oxidation of alpha-ketoglutarate is required for reductive carboxylation in cancer cells with mitochondrial defects. Cell Rep. 2014; 7: 1679–1690. https://doi.org/10.1016/j.celrep.2014.04.037 PMID: 24857658

43. DeBerardinis RJ, Cheng T. Q's next: the diverse functions of glutamine in metabolism, cell biology and cancer. Oncogene. 2010; 29: 313–324. https://doi.org/10.1038/onc.2009.358 PMID: 19881548

44. Spinelli JB, Yoon H, Ringel AE, Jeanfavre S, Clish CB, Haigis MC. Metabolic recycling of ammonia via glutamate dehydrogenase supports breast cancer biomass. Science. 2017; 358: 941–946. https://doi.org/10.1126/science.aam9305 PMID: 29025995

45. Leone RD, Zhao L, Englert JM, Sun I-M, Oh M-H, Sun I-H, et al. Glutamine blockade induces divergent metabolic programs to overcome tumor immune evasion. Science. 2019; 366: 1013–1021. https://doi.org/10.1126/science.aav2588 PMID: 31699883

46. Cheng T, Sudderth J, Yang C, Mullen AR, Jin ES, Matés JM, et al. Pyruvate carboxylase is required for glutamine-independent growth of tumor cells. Proc Natl Acad Sci U S A. 2011; 108: 8674–8679. https://doi.org/10.1073/pnas.1016627108 PMID: 21555572

47. Davidson SM, Papagiannakopoulos T, Olenchock BA, Heyman JE, Keibler MA, Luengo A, et al. Environment Impacts the Metabolic Dependencies of Ras-Driven Non-Small Cell Lung Cancer. Cell Metab. 2016; 23: 517–528. https://doi.org/10.1016/j.cmet.2016.01.007 PMID: 26853747

48. Singh B, Shamsnia A, Raythatha MR, Milligan RD, Cady AM, Madan S, et al. Highly Adaptable Triple-Negative Breast Cancer Cells as a Functional Model for Testing Anticancer Agents. PLOS ONE. 2014; 9: e109487. https://doi.org/10.1371/journal.pone.0109487 PMID: 25279830

49. Le A, Lane AN, Hamaker M, Bose S, Gouw A, Barbi J, et al. Glucose-independent glutamine metabolism via TCA cycling for proliferation and survival in B cells. Cell Metab. 2012; 15: 110–121. https://doi.org/10.1016/j.cmet.2011.12.009 PMID: 22225880

50. Yang C, Ko B, Hensley CT, Jiang L, Wasti AT, Kim J, et al. Glutamine Oxidation Maintains the TCA Cycle and Cell Survival during Impaired Mitochondrial Pyruvate Transport. Molecular Cell. 2014; 56: 414–424. https://doi.org/10.1016/j.molcel.2014.09.025 PMID: 25458842

51. Leithner K, Triebl A, Trötzmüller M, Hinteregger B, Leko P, Wieser BI, et al. The glycerol backbone of phospholipids derives from noncarbohydrate precursors in starved lung cancer cells. Proc Natl Acad Sci USA. 2018; 115: 6225–6230. https://doi.org/10.1073/pnas.1719871115 PMID: 29844165

52. Paudel BB, Harris LA, Hardeman KN, Abugable AA, Hayford CE, Tyson DR, et al. A Nonquiescent "Idling" Population State in Drug-Treated, BRAF-Mutated Melanoma. Biophys J. 2018; 114: 1499–1511. https://doi.org/10.1016/j.bpj.2018.01.016 PMID: 29590606

53. Jia D, Paudel BB, Hayford CE, Hardeman KN, Levine H, Onuchic JN, et al. Drug-Tolerant Idling Melanoma Cells Exhibit Theory-Predicted Metabolic Low-Low Phenotype. Front Oncol. 2020; 10: 1426. https://doi.org/10.3389/fonc.2020.01426 PMID: 32923395

54. Song C, Piva M, Sun L, Hong A, Moriceau G, Kong X, et al. Recurrent Tumor Cell-Intrinsic and -Extrinsic Alterations during MAPKi-Induced Melanoma Regression and Early Adaptation. Cancer Discov. 2017; 7: 1248–1265. https://doi.org/10.1158/2159-8290.CD-17-0401 PMID: 28864476

55. Stefan E, Bister K. MYC and RAF: Key Effectors in Cellular Signaling and Major Drivers in Human Cancer. Curr Top Microbiol Immunol. 2017; 407: 117–151. https://doi.org/10.1007/82_2017_4 PMID: 28466200

56. Nicklin P, Bergman P, Zhang B, Triantafellow E, Wang H, Nyfeler B, et al. Bidirectional Transport of Amino Acids Regulates mTOR and Autophagy. Cell. 2009; 136: 521–534. https://doi.org/10.1016/j.cell.2008.11.044 PMID: 19203585

57. Barrett T, Wilhite SE, Ledoux P, Evangelista C, Kim IF, Tomashevsky M, et al. NCBI GEO: archive for functional genomics data sets—update. Nucleic Acids Res. 2013; 41: D991–D995. https://doi.org/10.1093/nar/gks1193 PMID: 23193258

58. Luo M, Shang L, Brooks MD, Jiagge E, Zhu Y, Buschhaus JM, et al. Targeting Breast Cancer Stem Cell State Equilibrium through Modulation of Redox Signaling. Cell Metab. 2018; 28: 69–86.e6. https://doi.org/10.1016/j.cmet.2018.06.006 PMID: 29972798

59. Moussaieff A, Rouleau M, Kitsberg D, Cohen M, Levy G, Barasch D, et al. Glycolysis-Mediated Changes in Acetyl-CoA and Histone Acetylation Control the Early Differentiation of Embryonic Stem Cells. Cell Metab. 2015; 21: 392–402. https://doi.org/10.1016/j.cmet.2015.02.002 PMID: 25738455

60. Shyh-Chang N, Ng H-H. The metabolic programming of stem cells. Genes Dev. 2017; 31: 336–346. https://doi.org/10.1101/gad.293167.116 PMID: 28314766

61. Salmond RJ. mTOR Regulation of Glycolytic Metabolism in T Cells. Front Cell Dev Biol. 2018; 6: 122. https://doi.org/10.3389/fcell.2018.00122 PMID: 30320109

62. Ancey P-B, Contat C, Meylan E. Glucose transporters in cancer–from tumor cells to the tumor microenvironment. FEBS J. 2018; 285: 2926–2943. https://doi.org/10.1111/febs.14577 PMID: 29893496

63. Yoo HC, Yu YC, Sung Y, Han JM. Glutamine reliance in cell metabolism. Exp Mol Med. 2020; 52: 1496–1516. https://doi.org/10.1038/s12276-020-00504-8 PMID: 32943735

64. Calvert AE, Chalastanis A, Wu Y, Hurley LA, Kouri FM, Bi Y, et al. Cancer-associated IDH1 promotes growth and resistance to targeted therapies in the absence of mutation. Cell Rep. 2017; 19: 1858–1873. https://doi.org/10.1016/j.celrep.2017.05.014 PMID: 28564604

65. Kiesel VA, Sheeley MP, Coleman MF, Cotul EK, Donkin SS, Hursting SD, et al. Pyruvate carboxylase and cancer progression. Cancer Metab. 2021; 9: 20. https://doi.org/10.1186/s40170-021-00256-7 PMID: 33931119

66. Sarfraz I, Rasul A, Hussain G, Hussain SM, Ahmad M, Nageen B, et al. Malic enzyme 2 as a potential therapeutic drug target for cancer. IUBMB Life. 2018; 70: 1076–1083. https://doi.org/10.1002/iub.1930 PMID: 30160039

67. Ren J-G, Seth P, Clish CB, Lorkiewicz PK, Higashi RM, Lane AN, et al. Knockdown of Malic Enzyme 2 Suppresses Lung Tumor Growth, Induces Differentiation and Impacts PI3K/AKT Signaling. Sci Rep. 2014; 4: 5414. https://doi.org/10.1038/srep05414 PMID: 24957098

68. Scholnick P, Lang D, Racker E. Regulatory mechanisms in carbohydrate metabolism. IX. Stimulation of aerobic glycolysis by energy-linked ion transport and inhibition by dextran sulfate. J Biol Chem. 1973; 248: 5175–5182. https://doi.org/10.1016/S0021-9258(19)43686-7 PMID: 4268695

69. Ward PS, Thompson CB. Signaling in Control of Cell Growth and Metabolism. Cold Spring Harb Perspect Biol. 2012; 4: a006783. https://doi.org/10.1101/cshperspect.a006783 PMID: 22687276

70. Fang M, Shen Z, Huang S, Zhao L, Chen S, Mak TW, et al. The ER UDPase ENTPD5 promotes protein N-glycosylation, the Warburg effect, and proliferation in the PTEN pathway. Cell. 2010; 143: 711–724. https://doi.org/10.1016/j.cell.2010.10.010 PMID: 21074248

71. Israelsen WJ, Vander Heiden MG. ATP consumption promotes cancer metabolism. Cell. 2010; 143: 669–671. https://doi.org/10.1016/j.cell.2010.11.010 PMID: 21111226

72. Sakai H, Suzuki T, Maeda M, Takahashi Y, Horikawa N, Minamimura T, et al. Up-regulation of Na+,K +-ATPase α3-isoform and down-regulation of the α1-isoform in human colorectal cancer. FEBS Lett. 2004; 563: 151–154. https://doi.org/10.1016/S0014-5793(04)00292-3 PMID: 15063740

73. Kometiani P, Liu L, Askari A. Digitalis-Induced Signaling by Na+/K+-ATPase in Human Breast Cancer Cells. Mol Pharmacol. 2005; 67: 929–936. https://doi.org/10.1124/mol.104.007302 PMID: 15602003

74. Khajah MA, Mathew PM, Luqmani YA. Na+/K+ ATPase activity promotes invasion of endocrine resistant breast cancer cells. PLOS ONE. 2018; 13: e0193779. https://doi.org/10.1371/journal.pone.0193779 PMID: 29590154

75. Sanchez-Vega F, Mina M, Armenia J, Chatila WK, Luna A, La KC, et al. Oncogenic Signaling Pathways in The Cancer Genome Atlas. Cell. 2018; 173: 321–337.e10. https://doi.org/10.1016/j.cell.2018.03.035 PMID: 29625050

76. Sever R, Brugge JS. Signal Transduction in Cancer. Cold Spring Harb Perspect Med. 2015;5. https://doi.org/10.1101/cshperspect.a006098 PMID: 25833940

77. Monaco ME. Fatty acid metabolism in breast cancer subtypes. Oncotarget. 2017; 8: 29487–29500. https://doi.org/10.18632/oncotarget.15494 PMID: 28412757

78. Shah S, Carriveau WJ, Li J, Campbell SL, Kopinski PK, Lim H-W, et al. Targeting ACLY sensitizes castration-resistant prostate cancer cells to AR antagonism by impinging on an ACLY-AMPK-AR feedback mechanism. Oncotarget. 2016; 7: 43713–43730. https://doi.org/10.18632/oncotarget.9666 PMID: 27248322

79. Ware KE, Gupta S, Eng J, Kemeny G, Puviindran BJ, Foo W-C, et al. Convergent evolution of p38/MAPK activation in hormone resistant prostate cancer mediates pro-survival, immune evasive, and metastatic phenotypes. bioRxiv. 2020; 2020.04.22.050385. https://doi.org/10.1101/2020.04.22.050385

80. Bhattacharya D, Azambuja AP, Simoes-Costa M. Metabolic Reprogramming Promotes Neural Crest Migration via Yap/Tead Signaling. Dev Cell. 2020; 53: 199–211.e6. https://doi.org/10.1016/j.devcel.2020.03.005 PMID: 32243782

81. Marí M, Morales A, Colell A, García-Ruiz C, Fernández-Checa JC. Mitochondrial Glutathione, a Key Survival Antioxidant. Antioxid Redox Sign. 2009; 11: 2685–2700. https://doi.org/10.1089/ARS.2009.2695 PMID: 19558212

82. Bocci F, Tripathi SC, Vilchez Mercedes SA, George JT, Casabar JP, Wong PK, et al. NRF2 activates a partial epithelial-mesenchymal transition and is maximally present in a hybrid epithelial/mesenchymal phenotype. Int Bio (Cam). 2019; 11: 251–263. https://doi.org/10.1093/intbio/zyz021 PMID: 31329868

83. Faubert B, Li KY, Cai L, Hensley CT, Kim J, Zacharias LG, et al. Lactate Metabolism in Human Lung Tumors. Cell. 2017; 171: 358–371.e9. https://doi.org/10.1016/j.cell.2017.09.019 PMID: 28985563

84. Watson MJ, Vignali PDA, Mullett SJ, Overacre-Delgoffe AE, Peralta RM, Grebinoski S, et al. Metabolic support of tumour-infiltrating regulatory T cells by lactic acid. Nature. 2021; 1–7. https://doi.org/10.1038/s41586-020-03045-2 PMID: 33589820

85. Zappasodi R, Serganova I, Cohen IJ, Maeda M, Shindo M, Senbabaoglu Y, et al. CTLA-4 blockade drives loss of T reg stability in glycolysis-low tumours. Nature. 2021; 591: 652–658. https://doi.org/10.1038/s41586-021-03326-4 PMID: 33588426

86. Park JH, Vithayathil S, Kumar S, Sung P-L, Dobrolecki LE, Putluri V, et al. Fatty Acid Oxidation-Driven Src Links Mitochondrial Energy Reprogramming and Oncogenic Properties in Triple-Negative Breast Cancer. Cell Rep. 2016; 14: 2154–2165. https://doi.org/10.1016/j.celrep.2016.02.004 PMID: 26923594

87. Pudakalakatti SM, Uppangala S, D'Souza F, Kalthur G, Kumar P, Adiga SK, et al. NMR studies of pre-implantation embryo metabolism in human assisted reproductive techniques: a new biomarker for assessment of embryo implantation potential. NMR Biomed. 2013; 26: 20–27. https://doi.org/10.1002/nbm.2814 PMID: 22714820

88. Wishart DS, Tzur D, Knox C, Eisner R, Guo AC, Young N, et al. HMDB: the Human Metabolome Database. Nucleic Acids Res. 2007; 35: D521–526. https://doi.org/10.1093/nar/gkl923 PMID: 17202168